Magnetic-Field-Induced Second-Harmonic Generation in Semiconductor GaAs

V. V. Pavlov,[1] A. M. Kalashnikova,[1] R. V. Pisarev,[1] I. Sänger,[2] D. R. Yakovlev,[2,1] and M. Bayer[2]

[1]*A. F. Ioffe Physical-Technical Institute, The Russian Academy of Sciences, 194021 St. Petersburg, Russia*
[2]*Experimentelle Physik II, Universität Dortmund, 44221 Dortmund, Germany*
(Received 5 November 2004; published 22 April 2005)

We show that application of a magnetic field induces optical second-harmonic generation (SHG) in GaAs. This phenomenon arises from field-induced symmetry breaking causing new optical nonlinearities. A series of narrow SHG lines is observed in the spectral range from 1.52 to 1.77 eV that we attribute to Landau-level quantization of the band energy spectrum. The rotational anisotropy of the SHG signal distinctly differs from that of the electric-dipole approximation. Model calculations reveal that nonlinear magneto-optical spatial dispersion that comes together with the electric-dipole term is the dominant mechanism for this nonlinearity.

For more than half a century the linear and nonlinear optical properties of semiconductors have remained one of the most thriving fields of solid-state physics. Semiconductor optics provides fundamental information on the electronic and spin level structure and serves as the basis for numerous optoelectronic applications. Applied magnetic and electric fields, as well as strain, can radically modify the optical properties of semiconductors giving rise to a wealth of fascinating phenomena [1–3].

Among various *nonlinear* optical phenomena, second-harmonic generation (SHG) plays a particularly important role [4,5]. SHG in semiconductors has been the subject of continuing interest since the early years of nonlinear optics. However, it is still far from the state of maturity that has been achieved in *linear* optics. As a rule, SHG studies have been limited to singular wavelengths or narrow spectral ranges. Examples of SHG over a wide spectral range are scarce [6,7]. High spectral resolution, external magnetic fields, or low temperatures have not yet been exploited for SHG studies of semiconductors. As for applying the magnetic field, only one example is available for the rather weak SHG response of a silicon surface at a fixed frequency [8]. Theoretical calculations of crystallographic SHG susceptibilities can be found in literature [9–11], but for SHG in semiconductors subject to magnetic fields they are still missing.

In this Letter we report the observation of magnetic-field-induced SHG in GaAs. The magnetic field breaks the time-inversion symmetry and induces a new nonlinear response to the optical excitation. SHG spectra with well-defined polarization properties and characteristic magnetic-field and temperature dependencies are observed around the GaAs band gap. To explain this phenomenon we engage specific nonlinear processes for the interaction of light with the magnetized medium. We believe that these mechanisms of magnetic-field-induced SHG are also important for other semiconductors.

GaAs has been chosen for the present study as one of the most important semiconductors both for fundamental

physics and for manifold technological purposes. Recent publications show the continuing interest in the nonlinear optical properties of this material [7,12–14]. It crystallizes in the noncentrosymmetric structure of zinc-blende type with point group symmetry $\bar{4}3m$. In electric-dipole approximation the leading order SHG contributions in magnetic field $\mathbf{H}^0$ can be written as [5,15,16]

$$\mathbf{P}^{2\omega} \propto \chi^{eee}:\mathbf{E}^\omega\mathbf{E}^\omega + \chi^{eeem}:\mathbf{E}^\omega\mathbf{E}^\omega\mathbf{H}^0, \qquad (1)$$

where $\mathbf{P}^{2\omega}$ is the SHG polarization and $\mathbf{E}^\omega$ is the electric field at the fundamental frequency. Microscopically the nonlinear susceptibility χ^{eee} is given by the noncentrosymmetric part of the electric charge density. χ^{eee} is a polar third-rank tensor with nonvanishing components of type xyz (6) [17]. The crystallographic contribution $\chi^{eee}:\mathbf{E}^\omega\mathbf{E}^\omega$ has been investigated in several works [7].

In the present study the crystallographic contribution χ^{eee} was suppressed by a proper choice of the experimental geometry. For (001)-oriented GaAs χ^{eee} vanishes for normal light incidence, but χ^{eeem} gives a finite magnetic-field-induced contribution to SHG, which we study here. An axial fourth-rank tensor χ^{eeem} has nonvanishing components of type $xxyy(x{:}3) = -yyxx(y{:}3) = -xxzz(x{:}3) = zzxx(z{:}3) = yyzz(y{:}3) = -zzyy(z{:}3)$ [17]. This contribution is related to magnetic-field perturbations of the charge and spin distribution.

Three types of GaAs samples were investigated: (i) 10 μm gas-phase-epitaxy layers grown on semi-insulating GaAs (001) substrates [18], (ii) 2 μm epilayers grown by molecular-beam epitaxy, and (iii) (001)-oriented 0.5 mm thick platelets of bulk GaAs grown by the Bridgman method. Samples (i) have a defect density of 10^{14} cm^{-3}. For samples (ii) and (iii) it was $\sim 10^{15}$ cm^{-3}. In all samples the SHG spectra are very similar with respect to the spectral position of the observed features, although the intensities of the SHG peaks vary from sample to sample. Here we present experimental data for sample (i) only.

SHG spectra were recorded in transmission geometry using 8 ns light pulses with a 10 Hz repetition rate, generated by an optical parametric oscillator (OPO) pumped by the third harmonic of a solid-state Nd:YAG laser. The SHG signal was detected by a liquid nitrogen-cooled charged-coupled-device camera. A double pass monochromator and optical filters were used to suppress undesired luminescence. External magnetic fields up to 7 T were applied in the Voigt geometry perpendicular to the light wave vector: $\mathbf{H}^0 \parallel \mathbf{x}$ and $\mathbf{k}^\omega \parallel \mathbf{z}$. The sample temperature was varied from 6 up to 200 K.

Figure 1 shows SHG spectra for normal light incidence at $H = 7$ T for various configurations of the fundamental and SHG light polarizations. No crystallographic SHG signal is detected at zero field, confirming the suppression of the crystallographic contribution (see also Fig. 2). In the magnetic field the SHG signal appears consisting of a set of narrow lines in the spectral range from 1.515 to 1.77 eV for all three geometries. According to Eq. (1), only χ_{xyyx} components are allowed for $\mathbf{E}^{2\omega} \perp \mathbf{E}^\omega \parallel \mathbf{y}$ in Fig. 1(a). In the electric-dipole approximation no χ_{yyyx} SHG signal is expected for $\mathbf{E}^{2\omega} \parallel \mathbf{E}^\omega \parallel \mathbf{y}$. Surprisingly, for this geometry a strong SHG signal appears with an intensity that is 50 times larger than that for the dipole-allowed χ_{xyyx} contribution [Fig. 1(b)]. A weak signal was also found for the nominally forbidden χ_{yxxx} components, which are monitored in the geometry $\mathbf{E}^{2\omega} \perp \mathbf{E}^\omega \parallel \mathbf{x}$ in Fig. 1(c). Evidently, new mechanisms which overcome the limits

set by the electric-dipole approach have to be considered to explain the SHG signals in Figs. 1(b) and 1(c).

In the following we consider the properties of the strong χ_{yyyx} SHG signal as a function of magnetic field and temperature. The evolution of the SHG spectra in the magnetic field is shown in Fig. 2(a). With increasing field a set of narrow lines shifting from about 1.515 eV to higher energies and gaining in intensity appears. The intensity increase is proportional to H^2 as seen from the corresponding fit to the data for the strongest X line in the inset. As the SHG intensity $I^{2\omega} \propto |\mathbf{P}^{2\omega}|^2$, the nonlinear polarization $\mathbf{P}^{2\omega}$ must be a linear function of magnetic-field strength. The X linewidth of 2.0 meV, on the other hand, is independent of H (open circles in the inset). The peak positions vs magnetic field are plotted in Fig. 2(b), where the peak intensities are represented by the symbol sizes. Extrapolation of the peak energies to zero field gives 1.516 eV for the lowest line, which corresponds to the $1s$-exciton energy and about 1.519 eV for the other lines, which is the GaAs band gap energy at $T = 6$ K.

Application of a magnetic field to a semiconductor gives rise to quantization of the conduction and valence bands

FIG. 1. SHG spectra of GaAs measured for $\mathbf{k}^\omega \parallel \mathbf{z}$, $\mathbf{H}^0 \parallel \mathbf{x}$ in various geometries: (a) $\mathbf{E}^{2\omega} \perp \mathbf{E}^\omega \parallel \mathbf{y}$, (b) $\mathbf{E}^{2\omega} \parallel \mathbf{E}^\omega \parallel \mathbf{y}$, and (c) $\mathbf{E}^{2\omega} \perp \mathbf{E}^\omega \parallel \mathbf{x}$. Arbitrary units are used, but the ratio between ordinate axes is relevant. The amplitude of the background noise signal is about 0.1–0.2. The inset of (b) is the extension of the SHG spectrum towards higher energies.
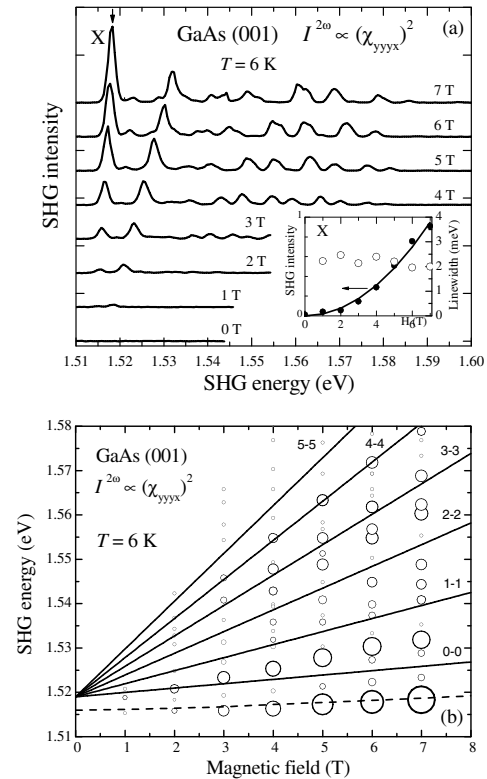
FIG. 2. (a) SHG spectra of GaAs at different magnetic fields. The inset shows the integrated SHG intensity and the linewidth of the strongest feature X vs magnetic field; the solid line is a H^2 fit to the intensity data. (b) Landau-level fan diagram of the SHG peak positions: dots are experimental data with intensities given by the symbol sizes. Solid lines give optical transition energies between Landau levels calculated from Eq. (2) for $N_e = N_h$. The dashed line gives the literature data for the diamagnetic shift of the $1s$ exciton state.

through the formation of Landau levels [19]. The electron-hole Coulomb interaction modifies the Landau-level spectrum leading to a rich magnetoexciton fan chart [20]. The diamagnetic shift for the 1s-exciton state given by the dashed line follows well the shift of the X line. A very rich spectrum of magnetoexcitons has been observed already in linear absorption experiments, and it is expected to be accomplished by new optically allowed transitions for the three-photon SHG. A detailed classification of lines in Fig. 2(b) is beyond the scope of this Letter, and we limit ourself to tracing the set of Landau-level transitions allowed for single photon absorption. The solid lines in Fig. 2(b) have been calculated by

$$E = E_g + \frac{e\hbar}{c}\left[\frac{1/2 + N_e}{m_e} + \frac{1/2 + N_h}{m_h}\right]H, \qquad (2)$$

where $E_g = 1.519$ eV is the GaAs band gap, $m_e = 0.067m_e$ and $m_{hh} = 0.51m_e$ are the electron and heavy-hole effective masses, and $N_e = N_h = 0, 1, 2, \dots$ are the Landau-level numbers. We do not account here for the exciton Zeeman splitting which does not exceed 1 meV below 7 T.

In Fig. 3 SHG spectra are shown for temperatures from 6 up to 200 K. The energy shift of the lines follows the temperature decrease of the GaAs band gap. Energies of the 1s exciton (circles) and the band gap (solid line) are compared in the upper inset. The dependencies of the integrated intensity and the linewidth of the 1s exciton on temperature are given in the lower inset. No particular activation energy can be assigned to the intensity decrease. Carrier scattering by phonons, perturbing the cyclotron motion, is one of the possible mechanisms for the SHG temperature variations. However, the SHG linewidth which should also increase by enhanced scattering does not vary with increasing temperature.

The rotational anisotropy of the SHG signal gives further insight into the nonlinear optical processes. SHG was recorded as a function of the azimuthal angle φ of the fundamental and the SHG polarization for the $\mathbf{E}^{2\omega} \parallel \mathbf{E}^{\omega}$ and $\mathbf{E}^{2\omega} \perp \mathbf{E}^{\omega}$ geometries (Fig. 4). The rotational anisotropy of the SHG intensity exhibits rather complicated twofold patterns. Moreover, none of these data can be modeled assuming only electric-dipole approximation [that is shown in Fig. 4(h)]. From these rotational anisotropy data different contributions to the SHG process can be disclosed.

The presence of a strong χ_{yyyx} SHG signal, which was supposedly forbidden, can be understood only if mechanisms different from the electric-dipole process are taken into account. Generally, the magnetic-field-induced contributions to the SHG can be written in a matrix form,

$$\begin{pmatrix} \mathbf{P}^{2\omega} \\ \mathbf{M}^{2\omega} \\ \mathbf{Q}^{2\omega} \end{pmatrix} \propto \begin{pmatrix} \chi^{eeem} & \chi^{eemm} & \chi^{emmm} \\ \chi^{meem} & \chi^{memm} & \chi^{mmmm} \\ \chi^{qeem} & \chi^{qemm} & \chi^{qmmm} \end{pmatrix} \begin{pmatrix} \mathbf{E}^{\omega} & \mathbf{E}^{\omega} & \mathbf{H}^0 \\ \mathbf{E}^{\omega} & \mathbf{H}^{\omega} & \mathbf{H}^0 \\ \mathbf{H}^{\omega} & \mathbf{H}^{\omega} & \mathbf{H}^0 \end{pmatrix}, \qquad (3)$$
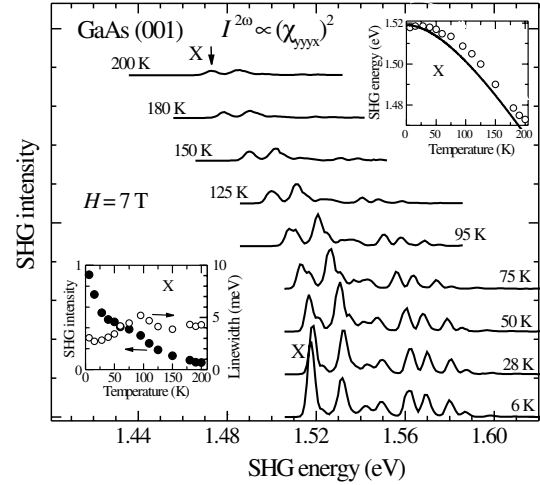
FIG. 3. SHG spectra of GaAs at different temperatures. Properties of the X line are presented in the insets. The energy shift of this line (circles) is compared with the GaAs band gap temperature dependence (line) in the upper inset. The integrated SHG intensity and linewidth are given in the lower inset.

where $\mathbf{H}^{\omega}$ is the magnetic field at the fundamental frequency, and $\mathbf{M}^{2\omega}$ and $\mathbf{Q}^{2\omega}$ denote magnetization and electric-quadrupole polarization at the SHG frequency. All nonlinear susceptibilities in Eq. (3) are allowed for the point group $\bar{4}3m$. However, the contributions with tensors χ^{emmm}, χ^{memm}, χ^{mmmm}, and χ^{qmmm} which relate three and four magnetic quantities, respectively, are believed to be very small. Moreover, the contribution involving the tensor χ^{qemm} most probably is very small also. The magnetic-dipole contributions of tensors χ^{eemm} and χ^{meem} and the electric-quadrupole contribution of tensor χ^{qeem} can be rewritten in a form that explicitly takes into account the nonlinear magneto-optical spatial dispersion

$$\mathbf{P}^{2\omega} \propto \chi^{eeekm} : \mathbf{E}^{\omega}\mathbf{E}^{\omega}\mathbf{k}^{\omega}\mathbf{H}^0, \qquad (4)$$

where χ^{eeekm} is an axial time-invariant fifth-rank tensor which has seven independent components. Using the transformation properties of the Cartesian coordinate system, the SHG intensities for the rotational anisotropies in the geometries $\mathbf{E}^{2\omega} \parallel \mathbf{E}^{\omega}$ and $\mathbf{E}^{2\omega} \perp \mathbf{E}^{\omega}$ can be written as

$$I_{\parallel}^{2\omega} \propto |(2A + C)\cos\varphi - D\sin\varphi\cos^2\varphi - (2A - B + C)\cos^3\varphi|^2, \qquad (5)$$

$$I_{\perp}^{2\omega} \propto |2D\cos\varphi - C\sin\varphi + (2A - B + C)\sin\varphi\cos^2\varphi - D\cos^3\varphi|^2. \qquad (6)$$

$A_{xxyzx} = A_{xyxzx}$, B_{yyyzx} and C_{yxxzx} are the spatial dispersion components of the tensor χ^{eeekm}, and $D_{xyyx} = -D_{yyxx} = -D_{yxyx}$ is the electric-dipole component of the tensor χ^{eeem} in Eq. (1). The experimental data for the rotational anisotropies in both geometries have been fitted by Eqs. (5) and (6), taking into account the complexity of the nonlinear
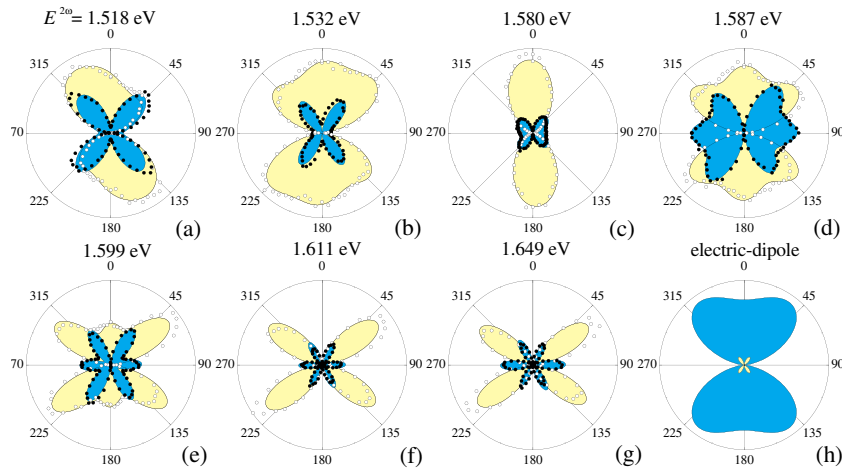
FIG. 4 (color online). Rotational anisotropies of the SHG intensities measured for GaAs for seven lines in the geometries $\mathbf{E}^{2\omega} \parallel \mathbf{E}^{\omega}$ (light shaded area) and $\mathbf{E}^{2\omega} \perp \mathbf{E}^{\omega}$ (dark shaded area). $T = 6$ K and $H = 7$ T. Experimental data are given by circles and shadow regions present results of modeling.

optical susceptibilities. This procedure gives a reliable set of fitting parameters for each photon energy and the results are shown in Fig. 4 by shaded areas. Good agreement between experimental and calculated SHG intensities is found for all rotational anisotropies, indicating that a combination of electric-dipole and spatial dispersion mechanisms is responsible for the observed nonlinear optical phenomena. The magnetic-field-induced Landau-level quantization leads to strong resonances in the density of states that enforce the higher order contributions to SHG. From them the nonlinear magneto-optical spatial dispersion with a characteristic length scale equal to the light wave vector $\mathbf{k}^{\omega}$ originates for this system.

In conclusion, magnetic-field-induced SHG has been observed in the nonmagnetic semiconductor GaAs. Landau-level magnetoexciton states play a key role in the SHG process. Model calculations involving electric-dipole and spatial dispersion mechanisms give an adequate description of the SHG rotational anisotropies. Nonlinear magneto-optical spatial dispersion turns out to be of crucial importance for the field-induced SHG. Our analysis is mostly based on symmetry considerations. We believe that the experiments will stimulate the development of a microscopic theory for deeper insight into the physical mechanisms involved. Recently we found the magnetic-field-induced SHG signal for semiconductor CdTe, also with a noncentrosymmetric crystal structure, which proves the general nature of the phenomena.

An application of SHG spectroscopy beyond the electric-dipole approach, in combination with external magnetic fields, opens new possibilities for studying electronic and spin structures of semiconductors and their heterostructures and may serve as supplementary and/or alternative tools to conventional linear optical methods. For example, the anisotropy patterns of the SHG with varying complexity for increasing energy might reflect the Bloch-function contributions to the involved Landau levels, so that insight into these functions (which otherwise are hardly accessible by optical means) might be taken.

[1] C. F. Klingshirn, *Semiconductor Optics* (Springer-Verlag, Berlin, 1995).

[2] P. Yu and M. Cardona, *Fundamentals of Semiconductors* (Springer-Verlag, Berlin, 1995).

[3] E. L. Ivchenko and G. E. Pikus, *Superlattices and Other Heterostructures. Symmetry and Optical Phenomena* (Springer-Verlag, Berlin, 1995).

[4] Y. R. Shen, *The Principles of Nonlinear Optics* (Wiley, New York, 1984).

[5] M. Fiebig, V. V. Pavlov, and R. V. Pisarev, J. Opt. Soc. Am. B **22**, 96 (2005).

[6] H. P. Wagner *et al.*, Phys. Rev. B **58**, 10 494 (1998).

[7] See, for example, S. Bergfeld and W. Daum, Phys. Rev. Lett. **90**, 036801 (2003), and references therein.

[8] V. Venkataramanan *et al.*, Appl. Phys. B **74**, 683 (2002).

[9] J. L. P. Hughes and J. E. Sipe, Phys. Rev. B **53**, 10 751 (1996).

[10] S. N. Rashkeev, W. R. L. Lambrecht, and B. Segall, Phys. Rev. B **57**, 3905 (1998).

[11] B. Adolph and F. Bechstedt, Phys. Rev. B **57**, 6519 (1998).

[12] T. Dekorsy *et al.*, Phys. Rev. Lett. **90**, 055508 (2003).

[13] Q. T. Vu *et al.*, Phys. Rev. Lett. **92**, 217403 (2004).

[14] A. Fiore *et al.*, Nature (London) **391**, 463 (1998).

[15] P. S. Pershan, Phys. Rev. **130**, 919 (1963).

[16] R. V. Pisarev *et al.*, Phys. Rev. Lett. **93**, 037204 (2004).

[17] R. R. Birss, *Symmetry and Magnetism* (North-Holland, Amsterdam, 1966).

[18] Yu. V. Zhilyaev *et al.*, Phys. Status Solidi (c) **0**, 1024 (2003).

[19] L. D. Landau and E. M. Lifshitz, *Quantum Mechanics* (Pergamon Press, Oxford, 1977).

[20] R. P. Seisyan and B. P. Zakharchenya, in *Landau Level Spectroscopy*, edited by G. Landwehr and E. I. Rashba (Elsevier Science, Amsterdam, 1991), Chap. 7.